

Chapter 12

Remote Sensing of Biological Soil Crusts at Different Scales

Bettina Weber and Joachim Hill

12.1 Introduction

Dryland ecosystems constitute some of the largest terrestrial biomes, collectively covering 41 % of Earth's land surface and supporting over 38 % of the global human population (Maestre et al. 2012). Biological soil crusts (biocrusts) often grow in patches, covering vast regions, making it impossible to accurately assess their spatial distribution patterns based on ground-based mapping techniques. Thus, remote sensing methods are invaluable to classify and characterize biocrusts and to analyze their alteration over time by means of remote sensing change detection analyses.

Remote sensing mapping techniques are based on the spectral characteristics of the studied features, in our case the biocrusts. Prior to developing a classification technique, the spectral patterns, which allow to distinguish between the biocrusts on the one and the underlying and adjoining substrates as well as the surrounding vegetation, on the other hand, need to be studied. Thus, this chapter is divided into two major parts: in the first part, the spectral reflectance properties of biological soil crusts are described and the effects of wetting and disturbance as well as the potential to deviate physiological characteristics from these spectral characteristics are discussed. In the second part, existing methodologies for biocrust classification are presented, their functionality is investigated, and finally their universal applicability and promising new methods for the future are discussed.

B. Weber (✉)

Multiphase Chemistry Department, Max Planck Institute for Chemistry, Hahn-Meitner-Weg 1,
55128 Mainz, Germany
e-mail: b.weber@mpic.de

J. Hill

Faculty of Regional and Environmental Sciences, Environmental Remote Sensing and
Geoinformatics, Trier University, 54286 Trier, Germany

12.2 Reflectance Spectroscopy of Biocrusts

12.2.1 Spectral Reflectance Characteristics of Biocrusts

The method of reflectance spectroscopy is based on electromagnetic radiation, which, according to the “wave” and the “particle model” can be described as an electromagnetic wave or as a particular kind of matter (Jensen 2007). According to the particle model, impacting energy causes the electrons of atoms to jump to a higher energy level (they are excited). After 10^{-8} s, the electrons fall back to the atoms’ lowest empty energy level, giving off radiation, which is a function of the energy that had been absorbed before. According to the quantum theory, this energy is released in discrete packets called quanta or photons. The energy of a quantum is inversely proportional to its wavelength, which is then measured by means of spectroscopy. Thus, the different colors of substances are caused by their differences in energy levels and the selection rules (Jensen 2007). Electron orbital changes are known to produce the shortest-wavelength radiation, near- and/or middle-infrared energy is caused by molecule vibrational motion, whereas long-wavelength infrared or microwave radiation is caused by rotational motion change (Jensen 2007). These spectral characteristics are measured as reflectance spectra displaying the amount of light reflected by a surface along different wavelengths.

As biocrusts comprise photosynthetically active organisms with chlorophyll, i.e., cyanobacteria, green algae, lichens, and mosses, one would expect to find the absorption maxima of chlorophyll within these spectra. In addition to that, the organisms may contain starch, cellulose, and additional pigments, which might be identified in the spectral response.

A general effect of lichen crusts on the variation of reflectance values of bare soils was already observed by Graetz and Gentle (1982), who worked on the reflectance characteristics of Australian semiarid rangelands. They, however, saw biocrusts more as a disturbing issue than as a noteworthy feature on their own.

12.2.1.1 Different Types of Biocrusts

The general spectral characteristics of biocrusts have been investigated in a number of studies, and in all of them, a chlorophyll absorption feature at a wavelength around 667–682 nm has been observed (Table 12.1). At 1450 and 1920 nm, a universal absorption caused by water or OH bonds was observed (Karnieli et al. 1999; Ustin et al. 2009). In the medium infrared region at ~2300 nm, Escribano et al. (2010) identified an additional adsorption feature in all biocrusts, which was assigned to the presence of lignin or cellulose.

In most studies, reflectance spectra of different biocrust types have been studied separately. Several studies revealed the overall reflectance values of cyanobacteria-dominated crusts to be lower throughout the spectrum (covering 400–2500 nm: O’Neill 1994; 400–900 nm: Weber et al. 2008; 350–1150 nm: Pinker and Karnieli 1995) as compared to bare soil. In contrast to that, other studies report lower

Table 12.1 Spectral characteristics of biocrusts as described in scientific publications

Crust type	Wavelength (nm)	Absorption feature	References	Opposing references
Cyanobacteria-dominated crust	~430	Increased reflectance due to phycobilins	Karnieli and Sarafis (1996)	Not observed by anybody else
Cyanobacterial strains of <i>Coleofasciculus chthonoplastes</i> and <i>Nostoc</i> sp.	~440	Absorption by chlorophyll <i>a</i> or β -carotene	Weber et al. (2008)	
Cyanobacterial strain of <i>Coleofasciculus chthonoplastes</i>	~489	Absorption by carotenoid or phycoerythrin	Weber et al. (2008)	
Cyanobacteria-dominated crusts	~504	Absorption by carotenoids	Chamizo et al. (2012), Rodríguez-Caballero et al. (2014)	
Cyanobacterial strain of <i>Coleofasciculus chthonoplastes</i>	~544	Absorption by phycocyanin or phycoerythrin	Weber et al. (2008)	Ustin et al. (2009)—no absorption in crusts
Cyanobacteria-dominated crust	<550	Higher reflectance than underlying soil	Tsoar and Karnieli (1996), Karnieli (1997)	Pinker and Karnieli (1995), O'Neill (1994), Weber et al. (2008), Chen et al. (2005)
Cyanobacteria-dominated crust	>550	Lower reflectance than underlying soil	Tsoar and Karnieli (1996), Karnieli (1997)	Pinker and Karnieli (1995), O'Neill (1994), Weber et al. (2008), Chen et al. (2005)
Cyanobacterial strain of <i>Coleofasciculus chthonoplastes</i>	~613	Absorption by phycocyanin	Weber et al. (2008)	Ustin et al. (2009)—no absorption in crusts
Cyanobacterial filaments of <i>Microcoleus</i> sp.	~627	Phycocyanin absorption	Karnieli et al. (2003)	
Cyanobacterial strains of <i>Coleofasciculus chthonoplastes</i> and <i>Phormidium</i> sp.	~630	Phycocyanin absorption	Weber et al. (2008)	

(continued)

Table 12.1 (continued)

Crust type	Wavelength (nm)	Absorption feature	References	Opposing references
Cyanobacteria-dominated crust; biocrusts in general	~680	Chlorophyll <i>a</i> absorption	O'Neill (1994), Pinker and Karnieli (1995), Karnieli and Tsoar (1995), Karnieli et al. (1996), Karnieli et al. (2002), Karnieli et al. (2003), Chen et al. (2005), Weber et al. (2008), Ustin et al. (2009), Escribano et al. (2010), Chamizo et al. (2012), Rodríguez-Caballero et al. (2014)	
All crust types	~1450	Water	Karnieli et al. (1999), Chamizo et al. (2012)	
Moss-dominated crust	~1720	Cellulose/lignin/starch/pectin	Karnieli et al. (1999)	
Moss- and lichen-dominated crusts	~1720	Cellulose and lignin	Ustin et al. (2009)	
Biocrust (not specified)	~1920	Water or –OH bonds	Karnieli et al. (1999), Ustin et al. (2009)	
Biocrust (not specified)	~2080	Cellulose, lignin, or other organic components (Escribano et al. 2010) or starch (O'Neill 1994)	O'Neill (1994), Ustin et al. (2009), Escribano et al. (2010)	Absorbing material doubted by Ustin et al. (2009)
Lichen-dominated crust	~2100	Starch and cellulose	O'Neill (1994)	
Moss-dominated crust	~2180	Starch/lignin/wax/tannin	Karnieli et al. (1999)	
Biocrust (not specified)	~2300	Lignin and cellulose	Escribano et al. (2010)	

(continued)

Table 12.1 (continued)

Crust type	Wavelength (nm)	Absorption feature	References	Opposing references
Moss-dominated crust	~2309	Humic acid/wax/starch	Karnieli et al. (1999)	Ustin et al. (2009)—absorption due to carbonate; observed in biocrusts and in soil

reflectance values at wavelengths between 550 and 1100 nm, whereas at shorter wavelengths (400–550 nm), higher reflectance values were measured on cyanobacteria-dominated crusts as compared to bare soil (Karnieli and Tsoar 1995; Tsoar and Karnieli 1996). Karnieli and Sarafis (1996) and later Karnieli et al. (1999) investigated the spectra of cyanobacteria-dominated biocrusts in an experimental approach, showing that phycobilins caused an increased reflectance of 1–2 % at about 430 nm. They claimed that this slightly increased reflectance may be used to differentiate between cyanobacteria-dominated crusts and bare soil and to classify cyanobacteria-dominated crusts within Landsat imagery (Karnieli 1997; see Sect. 12.3.2).

Reflectance spectra of isolated cyanobacterial strains revealed some additional absorption features, which could not be identified in complete crust samples (Table 12.1). On *Coleofasciculus chthonoplastes*, absorption maxima at ~440 nm (chlorophyll *a* or β -carotene), ~489 nm (carotenoid or phycoerythrin), ~544 nm (phycocyanin or phycoerythrin), ~613 nm (phycocyanin), and ~630 nm (phycocyanin) were determined by Weber et al. (2008). The absorption maximum at ~440 nm was shared by *Nostoc* sp., that at ~630 nm by *Phormidium* sp.. Karnieli et al. (2002) also observed the phycocyanin absorption maximum on *Microcoleus* filaments at ~627 nm.

On lichen-dominated biocrusts, the effect of chlorophyll, causing an absorption maximum between 670 and 680 nm, could be very weak (Chen et al. 2005), whereas in other cases it was clearly visible (Weber et al. 2008; Escribano et al. 2010). Further shallow absorption features at 2080 and 2100 nm were determined by O’Neill (1994), which he supposed to be caused by starch and a combination of starch and cellulose, respectively. The absorption feature at 2080 nm was also determined by Escribano et al. (2010), who ascribed it to the presence of cellulose, lignin, and/or other organic components.

In spectra of moss-dominated crusts, clear chlorophyll-conditioned absorption maxima were observed (Karnieli et al. 1999; Chen et al. 2005). Additional absorption features were identified at 1720 nm (assigned to cellulose, lignin, starch and/or pectin), 2180 nm (assigned to starch, lignin, wax and/or tannins), and at 2309 nm (assigned to humid acid, wax, and/or starch; Karnieli et al. 1999).

Weber et al. (2008) analyzed an additional type of liverwort-dominated biocrusts. Organisms of the dominating liverwort taxon *Riccia* have a dorsal “epithelium” of

achlorophyllous cells (Perold 1999), causing a silvery reflectance. Thus, this crust type revealed overall higher reflectance values with a chlorophyll absorption maximum being strongly masked.

12.2.1.2 Continuum Removal

The spectral characteristics of biocrusts as opposed to those of bare soil are often characterized by only subtle deviations. In order to identify such slight differences, Clark and Roush (1984) developed a method to model the continuum in a reflectance spectrum as a mathematical function, which is then used to isolate particular absorption features for analysis. This method was used by Escribano et al. (2010) to differentiate between crusts growing in different seasons, whereas Rodríguez-Caballero et al. (2014) illustrated an absorption peak at 504 nm caused by carotenoids, which was present in cyanobacteria, but did not occur in lichen-dominated crusts. Weber et al. (2008) applied continuum removal to set up five rules, which allowed to successfully delimitate biocrusts from both bare soil and vascular plant vegetation, which also proved to work reliably on hyperspectral remote sensing data (see Sect. 12.3.2).

In a later study, Chamizo et al. (2012) used this method to also set up rules, which allowed successful distinction between the spectral response of different crust types. This method was applied to spatial remote sensing data in a later approach (Rodríguez-Caballero et al. 2014).

12.2.2 Effects of Watering

Watering has an instantaneous effect on the reflectance spectra of lichen-dominated crusts, as illustrated by O'Neill (1994). Already 10 min after watering, the absorption maximum at ~680 nm had deepened, and also at wavelengths >1200 nm, reflectance values were considerably lower. Studying cyanobacteria-dominated crusts, also Karnieli and Sarafis (1996) observed overall lower reflectance values upon watering of the crust. After 12 h wet the reflectance at ~680 nm and around 1000 nm had decreased, probably caused by the movement of cyanobacteria within the crust (Danin 1991; Garcia-Pichel and Pringault 2001) or by the initiated growth and formation of new chlorophyll *a*. Analyzing cyanobacteria- and one moss-dominated crust in a dry state, 1 day and 7 days after watering and incubation, Karnieli et al. (1999) observed that the reflectance level decreased and a significant dip ~680 nm developed during the incubation process.

The spectral response following different watering regimes was also studied by Rodríguez-Caballero et al. (2015). Immediately after watering, the reflectance of a cyanolichen-dominated crust with non-lichenized cyanobacteria decreased considerably (Fig. 12.1). After 24 h, wet reflectance values within the visible part of the spectrum (400–700 nm) were below 4 % (Fig. 12.1) and the crust surface had turned dark (Fig. 12.2). Upon drying, the reflectance values increased again, reaching

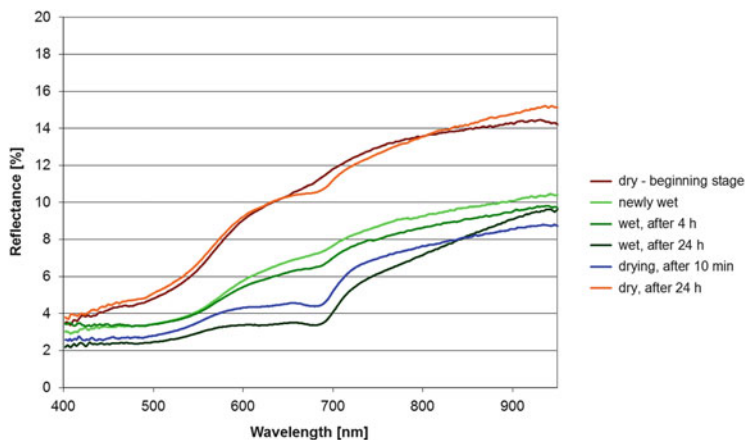


Fig. 12.1 Spectral response of a cyanolichen-dominated biocrust with cyanobacteria in a dry state and at different times during and after a 24-h watering event

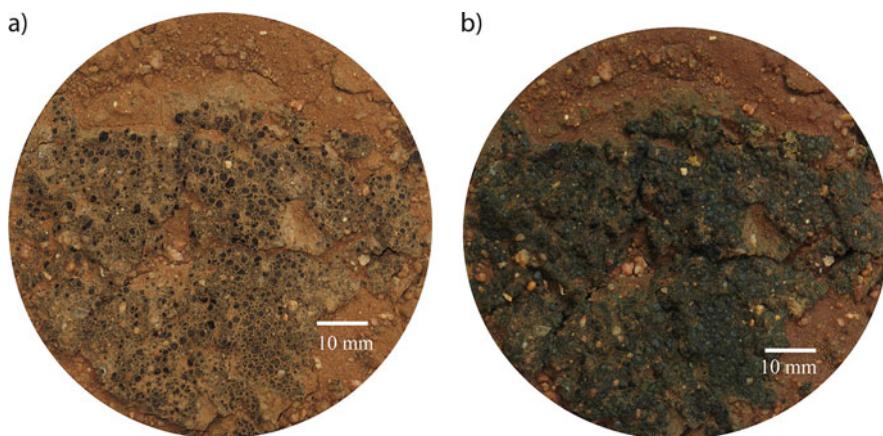


Fig. 12.2 Surface appearance of a cyanolichen-dominated biocrust with cyanobacteria (a) prior to watering, and (b) after 24 h in a wet stage

similar values over a major part of the spectrum, which remained, however, somewhat lower ~ 680 nm (Fig. 12.1), indicating the movement of organisms to the surface or the formation of new chlorophyll.

The spectral and optical response of cyanobacteria-dominated crusts after 10 days wet revealed considerable deviations from the former characteristics (Figs. 12.3 and 12.4b). The crust had turned almost blackish, indicating intense new growth of organisms, and after 1 day of subsequent drying, the overall spectral response was well below the initial spectrum with an intense reflectance minimum ~ 680 nm. During the subsequent 5 weeks of drying, the reflectance values increased gradually and the reflectance minimum ~ 680 nm flattened. Nevertheless,

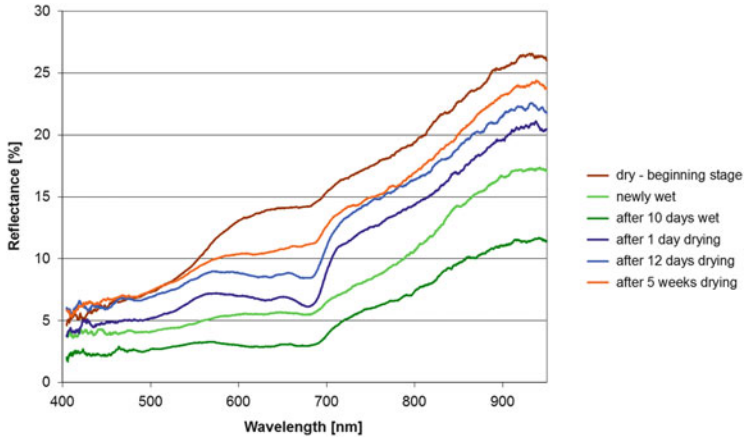


Fig. 12.3 Spectral response of a cyanolichen-dominated biocrust with cyanobacteria in a dry state and at different times during and after a 10-day watering event

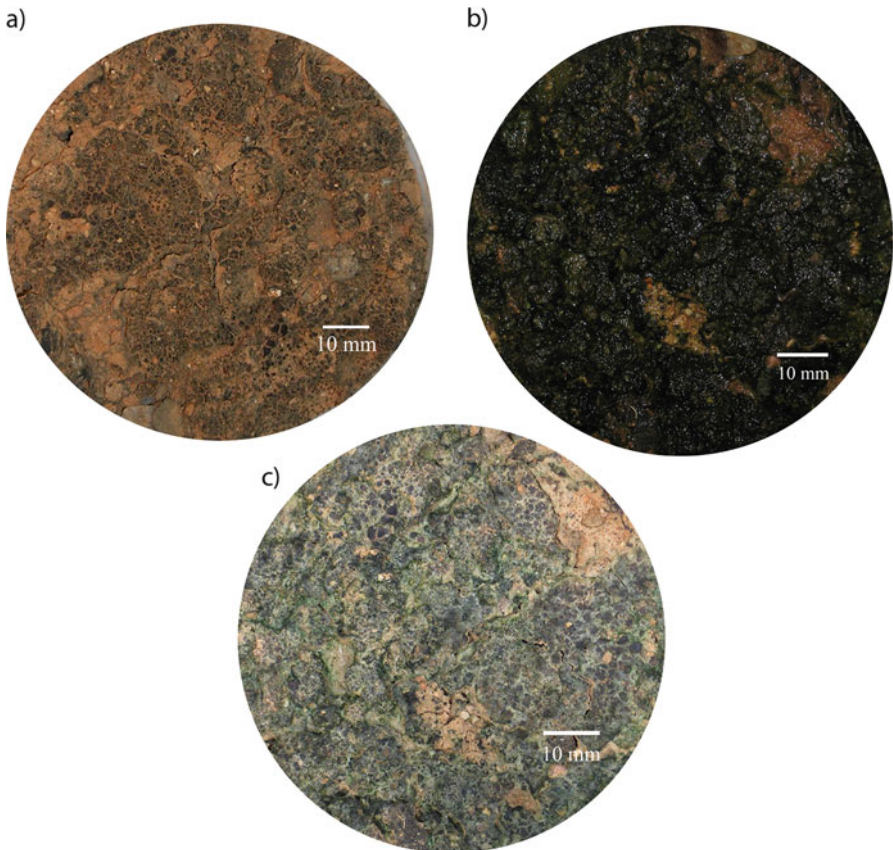


Fig. 12.4 Surface appearance of a cyanolichen-dominated biocrust with cyanobacteria (a) prior to watering, (b) in the end of 10-day watering event, and (c) 5 weeks (in a dry state) after 10-day watering event

reflectance values between 550 and 950 nm remained well below those of the initially measured spectrum and the crust looked still more densely colonized compared to the initial crust habitus (Figs. 12.3 and 12.4a, c). Thus, watering of the crusts over several days seems to have a long-term effect on the spectral characteristics of biocrusts.

Karnieli et al. (2002) studied the spectral reflectance of biocrusts depending on rainy and dry seasons during the year. After 2 weeks of rainfall, they measured well-developed reflectance spectra reminding of vascular plants with a high peak at ~550 nm, a distinct absorption maximum at ~680 nm, a sharp rise at ~700 nm (red edge), and a plateau in the near-infrared (700–1100 nm). During the following dry season the spectrum flattened, the maxima and minima gradually disappeared, and at the end of the dry season the spectra closely resembled those of bare soil (Karnieli et al. 2002). In a different study, biocrusts ($n=5$), which had been collected after the rainy season, were stored for 11 months under dry conditions in the dark. The spectral reflectance of the crusts did not change significantly over the whole time span (Weber unpublished), pointing to the fact that sunlight and/or UV-radiation might be responsible for the spectral alteration of biocrusts during the year.

12.2.3 Effects of Disturbance on the Spectral Characteristics of Biocrusts

Whereas biocrusts generally cause a darkening of the soil surface, their disturbance by both trampling and scraping provokes an increase in albedo (Chamizo et al. 2012). As trampling causes a breakdown of the crust, the lighter-colored soil becomes more dominant in reflectance spectra and after scraping, the spectra closely resemble these of bare soil. Absorption features of pigments ~500 and ~680 nm and of water ~1450 nm were observed to be weaker in trampled and weakest in scraped crusts. A second disturbance effect is the flattening of the surface by both trampling and scraping, also resulting in increased reflectance values (Chamizo et al. 2012).

Mechanical substrate disturbance had similar effects in a study by Ustin et al. (2009), where biocrusts responded with overall higher reflectance values and shallower absorption features at ~420 and ~500 nm. An absorption feature at ~2080 nm, probably caused by organic components, disappeared completely upon disturbance (Ustin et al. 2009).

12.2.4 Spectral Indicators

As previously shown, biocrusts have an absorption feature at ~680 nm in common (Table 12.1), which nicely correlates with the chlorophyll content of dry cyanobacteria-, lichen-, and moss-dominated crusts in a savannah-type ecosystem in Namibia (BIOTA observatories 39, 40; Weber unpublished; Fig. 12.5). This chlorophyll *a* absorption feature is also utilized in vegetation indices, with the most prominent one being the normalized difference vegetation index (NDVI). The NDVI is based on the spectral reflectance of Landsat satellite bands, i.e., the red band (*R*), 600–700 nm, comprising the chlorophyll absorption, and the near-infrared band (NIR), covering 700–1100 nm. It is defined as

$$\text{NDVI} = (\text{NIR} - R) / (\text{NIR} + R)$$

reaching values between -1 and 1 .

It was observed that wet cyanobacteria-dominated crusts on sand reached NDVI values up to 0.22 and moss-dominated crusts even gained values of 0.3 (Karnieli et al. 1996, 1999), whereas bare soil had values of 0.08. Thus, they showed that high NDVI values of wet biocrusts may be misinterpreted as vascular plant vegetation dynamics, whereas dry biocrusts only gained negligible NDVI values.

Zaady et al. (2007) used a brightness index (BI) in addition to the NDVI to follow the biocrust succession after a disturbance event. The BI utilizes the reflectance values in the green (*G*: 500–600 nm), red (*R*: 600–700 nm), and near-infrared region (NIR: 700–1100 nm) to calculate the overall brightness of a surface:

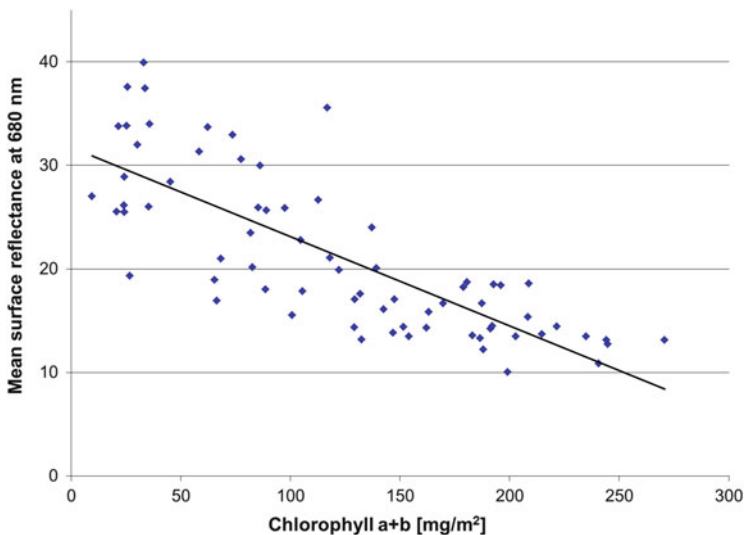


Fig. 12.5 Correlation of mean surface reflectance at 680 nm with chlorophyll *a+b* content of dry cyanobacteria-, lichen-, and moss-dominated crusts sampled in a savannah-type ecosystem in the BIOTA observatories No. 39 and 40 in Namibia. Pearson: $r = -0.78$, $n = 71$

$$BI = \sqrt{G^2 + R^2 + NIR^2}$$

In 6 years after disturbance by scraping, with the crumbled soil being distributed again, the brightness index decreased and the NDVI values increased as expected, but the same development, to a lesser extent, also occurred on non-disturbed control plots. The NDVI values of the controls were significantly higher than those of the treatment plots, but nevertheless, only comparably low NDVI values up to 0.15 were measured on wet crusts.

12.2.5 Spectral Characteristics Related to CO₂ Gas Exchange

As the spectral reflectance at ~680 nm correlates with the chlorophyll content of biocrusts, Burgheimer et al. (2006a, b) investigated the feasibility to derive carbon flux rates from NDVI values of biocrusts. This worked quite well when average data of each 3-day field trip were used. At higher temporal resolution, however, environmental factors like soil water content and light intensity strongly influenced CO₂-gas exchange values, whereas NDVI values remained stable. Thus, only weak correlations were found between both factors measured on biocrusts growing in sandy ($R^2 = 0.44$) and in loess environment ($R^2 = 0.35$; Burgheimer et al. 2006b). Nevertheless, the NDVI was found to be a good tool to represent the biocrusts' seasonal photosynthetic activity. Thus, in a later step, remote sensing methods might be applicable to estimate biocrust assimilation activity (Burgheimer et al. 2006a).

In another approach, chlorophyll fluorescence measurements of cyanobacteria-, lichen-, and moss-dominated crusts were linked to the NDVI and photochemical reflectance index (PRI; Yamano et al. 2006). The PRI is sensitive to changes in carotenoid pigments, which in turn are indicative of photosynthetic light use efficiency. It is calculated as

$$PRI = (R_{531} - R_{570}) / (R_{531} + R_{570})$$

with R indicating reflectance and numbers indicating the wavelengths in nanometers. Whereas the NDVI values of wet samples were higher in wet as compared to dry crusts, PRI values of wet crusts had lower values compared to dry ones. Due to inactivity of the crusts, no F_v/F_m was measured on dry crusts. In hydrated moss-dominated crusts, PRI values significantly correlated with F_v/F_m and in wet lichen-dominated crusts F_v/F_m was positively correlated with both the PRI and the NDVI. The authors concluded that the PRI was more effective in estimating the photosynthetic capacity of lichen- and moss-dominated crusts. One, however, has to have in mind that realized CO₂ gas exchange values cannot be directly derived from the fluorescence data measured on the crusts (Raggio et al. 2014).

12.3 Mapping the Spatial Distribution of Biocrusts

Given the significant role of biocrusts in assuring the functioning of desert and steppe ecosystems, there has always been a strong interest in producing spatially explicit distribution maps for improving the estimates of photosynthetic activity and CO₂ exchange retrieved from limited ground measurements (Burgheimer et al. 2006a). The fact that biomass and activity in biological soil crusts are usually concentrated within the uppermost millimeters of the soil surface (see Chap. 13 by García-Pichel et al.) suggests that, in case stable relationships between optically active key variables and crust properties are identified, satellite-based or airborne remote sensing might be employed to assess the presence or absence of biological soils crusts or to differentiate between various crust types (e.g., Karnieli et al. 2003).

While only very limited work has been done on the emissive properties of biocrusts (e.g., Rozenstein and Karnieli 2014), a wealth of studies is available on the use of imaging systems which operate in the reflective optical domain. Already at the time of early Landsat satellites during the 1970s, the nature of the sharp contrast along the Israel–Egypt border has been a matter of scientific interest and debate. Otterman et al. (1974) were the first to explain this by the presence of dark desert plants (either photosynthetically active or senescent) on the Israeli side, while the Egyptian area was almost devoid of vegetation. However, the predominant role of higher plants in producing this spectral contrast was rejected by Karnieli and Tsoar (1995) who claimed that the spectral contrast was not a direct result of vegetation cover but caused by an almost complete presence of biogenic crusts. In his reply Otterman (1996) insisted that even with sparse plant cover (e.g., less than 30 %), the interception of solar irradiance by desert plants, as well as the rays reflected from the soil (i.e., absorption and shadowing), is providing a highly significant contribution to the spectral reflectance.

Besides the fact that the presence of biocrusts in this area is by far more discontinuous and scattered than it was suggested in former studies (Hill et al. 2008), this early scientific debate frames the core problem of mapping biocrusts with multi- or hyperspectral imaging systems: biocrusts are mostly associated with higher plants, and the problem emerging from this fact is that the observed reflectance signal represents a more or less complex mixture of spectral contributions from soil, biocrusts, and vascular plants in varying states and, therefore, partially similar reflectance characteristics. In addition, the contribution biocrusts have on spectral soil surface properties does not depend only on crust composition and state but also on their relative cover (Rodríguez-Caballero et al. 2014). The task is thus to identify different types of biocrusts and to quantify their relative abundance at sub-pixel scale against the background of spectrally similar components.

12.3.1 *Image Preprocessing*

Monitoring of vegetation and land surface characteristics using passive optical imaging systems largely depends on relationships between biophysical quantities on the ground and their spectral reflectance properties. The different approaches for mapping biological soils crusts discussed in this chapter rely on the availability of calibrated reflectance imagery, i.e., they require that effects of the atmosphere, sun, and sensor positions as well as surface orientation have been properly corrected. The use of atmospheric radiative transfer models to remove atmospheric effects from Landsat imagery has recently been demonstrated in an operational context by a number of authors, such as Richter and Schläpfer (2002), Masek et al. (2006), Vicente-Serrano et al. (2008), and Flood et al. (2013). Since these concepts can be equally applied to a large variety of multispectral imaging systems and are currently included in operational data processing schemes, atmospheric corrections should be considered a necessary prerequisite that can be solved routinely.

12.3.2 *Spectral Indices*

The work in establishing suitable mapping methods builds on the spectral characteristics of biocrusts which are described in more detail in the first part of this chapter. Accordingly, the prominent chlorophyll absorption feature at ~680 nm, common to cyanobacteria-, lichen-, and moss-dominated crusts, might suggest the use of corresponding ratio indices such as the NDVI. However, since NDVI values in the range of 0.05–0.25 are also typical for a wide range of soil spectra, and because sparse woody vegetation structures as well tend to become spectrally effective from NDVI values around 0.1–0.15 onwards (e.g., Price 1993), this would require that the contribution of such materials to the reflectance signal could be computationally removed.

Karnieli (1997) was one of the first authors to propose a simple spectral index which was based on findings that the presence of cyanobacteria in the biocrusts is the cause for a relatively high reflectance in the blue region. He demonstrated that the spectral index

$$CI = 1 - \frac{\rho_{\text{red}} - \rho_{\text{blue}}}{\rho_{\text{red}} + \rho_{\text{blue}}}$$

had the ability to differentiate between crusted and uncrusted samples in laboratory experiments. Since the CI can also be derived from any imaging system with spectral bands in the blue and red region of the electromagnetic spectrum (e.g., the Landsat systems, MODIS, or the forthcoming Sentinel-2 and -3 systems), it suggested a wide range of applicability. However, the major problem was that the index enhances the spectral contrast between different geomorphic and lithological

units (e.g., areas with different mineralogies and varying contents of fine-grained material or organic components) in general, but fails to provide a reproducible relationship with increasing biocrust abundance. In addition, the index would by definition be less suitable for biological soil crusts where cyanobacteria are not a dominant constituent (Chen et al. 2005). The obvious conclusion to be drawn is to not only identify spectral ranges which are sensitive to varying abundances of biocrusts but to combine these with bands that are suited to enhance the spectral difference between biological crusts and associated material such as bare soil and photosynthetically active, senescent, or woody plant material.

Based on a study in the cold deserts of N-China, Chen et al. (2005) developed a biological soil crust index (BSCI) which is based on the reflectance in the green, red, and near-infrared range of the electromagnetic spectrum. The proposed index

$$\text{BSCI} = \frac{1 - L \cdot |\rho_{\text{red}} - \rho_{\text{green}}|}{\rho_{\text{AVE}}}$$

uses the average reflectance in the red, green, and near-infrared bands (ρ_{AVE}) to normalize the spectral contrast between the red and green part of the spectrum; L is an adjustment parameter to amplify the absolute difference between these bands. The rationale behind the BSCI is that the red reflectance for biological soil crusts will be much lower than those of bare sand, dry plant material, or photosynthetic vegetation. Chen et al. (2005) demonstrated that the performance of the proposed BSCI is limited to specific bounds, and that these can be substantially extended when atmospherically corrected imagery is used. However, an important limitation of the BSCI is that it must be applied under conditions where higher plants exhibit no photosynthetic activity.

The BSCI had been developed for a specific crust type (with a dominance of lichens) and it was therefore not surprising that transferring the index to a different site in S-Africa was not successful (Weber et al. 2008). However, the availability of hyperspectral imagery (CASI) with a spatial resolution of 1 m allowed the authors to analyze the spectral information content of field-measured biocrust spectra in more detail. Hyperspectral sensors can identify subtle spectral characteristics related to the presence of chlorophyll, carotenoids, and phycobilins in biocrusts (Rodríguez-Caballero et al. 2014). Weber et al. (2008) identified subtle but characteristic differences within the absorption regions around 516 and 675 nm which could be used to define a hyperspectral Continuum Removal Crust Identification Algorithm (CRCIA). When applying this index to hyperspectral CASI data, it was possible to map biological soil crusts as long as those covered more than approximately 30 % per pixel.

The importance of high spectral resolution has been acknowledged in several studies (e.g., Hill et al. 1999; Pinet et al. 2006; Escribano et al. 2010), particularly because additional diagnostic bands in the short-wave infrared region (due to the presence of cellulose, lignin, and other organic components) may support discrimination between biocrusts and soils. Also Ustin et al. (2009) confirmed the important

potential of hyperspectral imagery, since they could identify experimental treatments of biological soil crusts as part of a long-term manipulative experiment. However, it is important to understand that these treatments were applied to homogeneous plots, where the interaction with other materials was largely excluded.

More complicated is the identification when biocrusts are mixed with other soil properties or higher plants. The CRCIA, for example, worked quite reliably also in the presence of plant litter. However, it was observed that spectra of bare soil with minor photosynthetic plant coverage (about 5–10 %) already closely resemble certain types of biocrusts. This implies that biological crusts are almost impossible to map when growing in the proximity of, or even below, photosynthetic shrubs. For this reason an application of the CRCI algorithm on images with coarser spatial resolution was considered critical, owing to increasing spectral mixing effects in the visible and near-infrared (Weber et al. 2008). Similarly, important spectral features of dry and woody plant material (cellulose, starch, etc.) in the 2–2.5 μm wavelength range are also common to certain types of biocrusts. It should therefore not be expected that the availability of hyperspectral data alone can resolve all spectral ambiguities when biocrusts occur spatially mixed with desert plants in photosynthetic or non-photosynthetic states.

12.3.3 *Biocrusts as an Element of Complex Spectral Mixtures*

In principle the work of Chen et al. (2005) and Weber et al. (2008) already conceptualized the detection of biocrusts as a spectral mixing problem (where biological soil crusts and a background consisting of bare sand, green, or dry plant material and its shadow are main components of the composite reflectance). However, instead of developing optimized spectral indices it might be appropriate to adopt approaches for directly estimating the proportional abundance of materials within an observed surface area. Spectral mixture analysis (SMA) has been advocated as an efficient method to computationally decompose spectra into proportions of pure spectral components (endmembers; e.g., Schowengerdt 1997; Smith et al. 1990). In first approximation, spectral mixing is modeled as a linear combination of pure component (“endmember”) spectra:

$$\rho_i = \sum_{j=1}^n F_j \cdot \rho E_{ij} + \varepsilon_i$$

where ρ_i is the reflectance of the mixed spectrum in band i , ρE_{ij} is the reflectance of the endmember spectrum j in band i , F_j denotes the abundance of endmember j , and ε_i is the residual modeling error in band i .

Maps of endmember abundances F_j provide the convenience and inter-comparability of standard land cover metrics (e.g., NDVI) while retaining benefits

of physically based estimates, and they can be edited and recombined to produce thematic maps. Hill et al. (2008), for example, could successfully demonstrate that SMA was capable to differentiate between important surface materials (sand, biocrusts, and mineral crusts with different silt/clay contents) on reflectance-calibrated high-spatial-resolution true-color air photos after these had been stratified into areas with and without higher plant coverage. When SMA was applied to hyperspectral imagery, the analysis of mixing residuals (which usually indicate components not represented by the set of endmembers) proved that, in addition to the occurrence of biocrusts, also senescent and woody plants were an essential part of the composite reflectance of the Nizzana dune system in Israel (Hill et al. 1999), thereby confirming the results of Otterman (1996).

Recently, Rodríguez-Caballero et al. (2014) combined a support vector machine classification of hyperspectral CASI data in five ground units (dominated by principal surface components, such as bare soil, green, and dry vegetation, cyanobacteria, and lichen biocrusts) with an analysis of the SMA-derived abundance of different crust types within these units. It was found that all SMA models with a fixed number of spectral endmembers had limited performance (large root-mean-squared modeling errors and/or substantial amounts of abundance estimates smaller than 0 or larger than 100 %), independently of being applied either to the entire image or to more homogeneous ground units. This represents a common problem with linear SMA; it typically occurs when the number of spectral endmembers is greater than the number actually required to unmix an individual pixel in the scene. Material abundances predicted by linear SMA are therefore most accurate when only those endmembers that comprise a given pixel are used. It has therefore been suggested to replace simple SMA by efficient multiple endmember concepts which include the automatic detection of required endmembers (e.g., García-Haro et al. 2005; Rogge et al. 2006). Correspondingly, the application of multiple endmember SMA (MESMA) to pre-stratified ground units in the study of Rodríguez-Caballero et al. (2014) helped to improve results substantially.

12.3.4 Temporal Variability

All methods referred to so far cannot fully resolve the fundamental problem that, depending on the seasonal and short-term variability of phenological conditions, biocrusts may adopt reflectance properties very similar to soils or higher plants of steppe or desert ecosystems. The analysis of an exceptionally long observation record (28 satellite images from two consecutive years) with corresponding field data enabled Burgheimer et al. (2006a) to present a detailed analysis of the spectral reflectance dynamics of cyanobacteria-dominated biocrusts and other ground features in the northern Negev Desert in Israel (Burgheimer et al. 2006a). Although both the photosynthetic activation of biocrusts and the growth of annual plants are triggered by rainfall events during the winter period, it could be demonstrated that

biocrusts and annuals (although spectrally similar) might become separable due to different development rates: biocrusts are responding almost immediately to the availability of water while the emergence of annual plants is slower. Spatial separation of the two will thus depend on the availability of satellite observations during the time span where biocrusts are photosynthetically active but annuals have not yet reached a cover proportion high enough to mask the biocrust reflectance. This period, however, is short (usually not more than 2 weeks) and requires the availability of earth observation systems that combine suitably high spatial resolution with sufficiently high repetition rates. Such systems in principle exist (e.g., the RapidEye, SPOT, and WorldView multi-satellite constellations), but their acquisition management needs to efficiently cope with highly irregular rainfall and diverse temperature regimes common to semiarid and arid ecosystems. The high variability of different biocrust types (i.e., cyanobacteria-, lichen-, or moss-dominated), which frequently will be found associated to or mixed with each other, adds additional complications which render also the exploitation of such multi-temporal observation schemes anything else than trivial.

12.4 Conclusion

Biocrusts are spectrally characterized by a chlorophyll *a* absorption feature at ~680 nm accompanied by spectral features varying between biocrust types, substrates, and studies. Watering causes a rapid intensification of spectral characteristics, whereas disturbance was observed to produce overall higher albedo and flattened absorption features. Few studies showed that spectral indices may also be used to draw conclusions on the photosynthetic potential of biocrusts, but here further studies are needed to evaluate the overall explanatory power of spectral data.

Improving the production of reliable maps of biocrust cover further depends on the availability of imaging systems which provide not only adequate spatial and spectral resolution but are also capable of collecting images sufficiently frequent. Owing to the irregular rainfall regimes in global drylands, short repetition cycles are required to provide observations within the unusually short phenological windows when the spectral contrast between biocrusts and background components is maximized.

This primarily qualifies airborne imaging or, alternatively, space systems which build on multi-satellite constellations for implementing sufficiently dense repetition rates, such as RapidEye (<http://blackbridge.com/rapideye/>), the SPOT-6/7 and WorldView constellations (<http://www.satimagingcorp.com/>), and others. Since 2015 onwards the European Sentinel-2 satellite complements Landsat-8 OLI and forms an additional, powerful EO constellation which covers the visible and near- and short-wave infrared region at intermediate spatial resolution. Hyperspectral information seems able to capture also the more subtle spectral variability of biocrusts and vascular plants during the phenological cycle. Acquiring

hyperspectral images at least twice a year is expected to further improve monitoring capabilities. The German hyperspectral EnMAP mission scheduled for launch in 2018 (<http://www.enmap.org/>) will add important monitoring capacities.

Acknowledgments BW gratefully acknowledges support by the Max Planck Society (Nobel Laureate Fellowship) and the German Research Foundation (projects WE2393/2-1 and WE2393/2-2).

References

- Burgheimer J, Wilske B, Maseyk K, Karnieli A, Zaady E, Yakir D, Kesselmeier J (2006a) Ground and space spectral measurements for assessing the semi-arid ecosystem phenology related to CO₂ fluxes of biological soil crusts. *Remote Sens Environ* 101:1–12
- Burgheimer J, Wilske B, Maseyk K, Karnieli A, Zaady E, Yakir D, Kesselmeier J (2006b) Relationships between Normalized Difference Vegetation Index (NDVI) and carbon fluxes of biologic soil crusts assessed by ground measurements. *J Arid Environ* 64:651–669
- Chamizo S, Stevens A, Canton Y, Miralles I, Domingo F, Van Wesemael B (2012) Discriminating soil crust type, development stage and degree of disturbance in semiarid environments from their spectral characteristics. *Eur J Soil Sci* 63:42–53
- Chen J, Zhang MY, Wang L, Shimazaki H, Tamura M (2005) A new index for mapping lichen-dominated biological soil crusts in desert areas. *Remote Sens Environ* 96:165–175
- Clark RN, Roush TL (1984) Reflectance spectroscopy—quantitative-analysis techniques for remote-sensing applications. *J Geophys Res* 89:6329–6340
- Danin A (1991) Plant adaptations in desert dunes. *J Arid Environ* 21:193–212
- Escribano P, Palacios-Orueta A, Oyonarte C, Chabrilat S (2010) Spectral properties and sources of variability of ecosystem components in a Mediterranean semiarid environment. *J Arid Environ* 74:1041–1051
- Flood N, Danaher T, Gill T, Gillingham S (2013) An Operational Scheme for Deriving Standardised Surface Reflectance from Landsat TM/ETM+ and SPOT HRG Imagery for Eastern Australia. *Remote Sens* 5:83–109
- García-Haro FJ, Sommer S, Kemper T (2005) A new tool for variable multiple endmember spectral mixture analysis (VMESMA). *Int J Remote Sens* 26:2135–2162
- García-Pichel F, Pringault O (2001) Microbiology—cyanobacteria track water in desert soils. *Nature* 413:380–381
- Graetz RD, Gentle MR (1982) The relationships between reflectance in the Landsat wavebands and the composition of an Australian semi-arid shrub rangeland. *Photogramm Eng Remote Sens* 48:1721–1730
- Hill J, Udelhoven T, Schütt B, Yair A (1999) Differentiating biological soil crusts in a sandy arid ecosystem based on multi- and hyperspectral remote sensing data. In Schaeppmann M, Schläpfer D, Itten K (eds) Proceedings of the 1st EARSEL workshop on imaging spectroscopy, Zürich, 6–8 Oct 1998. Paris, pp 427–436
- Hill J, Udelhoven T, Jarmer T, Yair A (2008) Land cover in the Nizzana sandy arid ecosystem. Mapping surface properties with multi-spectral remote sensing data. In: Breckle S-W, Yair A, Veste M (eds) *Arid dune ecosystems: the Nizzana sands in the Negev desert*, vol 200, Ecological studies. Springer, Berlin, pp 157–172
- Jensen JR (2007) *Remote sensing of the environment: an earth resource perspective*, 2nd edn. Pearson Prentice Hall, Upper Saddle River, NJ
- Karnieli A (1997) Development and implementation of spectral crust index over dune sands. *Int J Remote Sens* 18:1207–1220
- Karnieli A, Sarafis V (1996) Reflectance spectrophotometry of cyanobacteria within soil crusts - A diagnostic tool. *Int J Remote Sens* 17:1609–1614

- Karnieli A, Tsoar H (1995) Spectral reflectance of biogenic crust developed on desert dune sand along the Israel Egypt border. *Int J Remote Sens* 16:369–374
- Karnieli A, Shachak M, Tsoar H, Zaady E, Kaufman Y, Danin A, Porter W (1996) The effect of microphytes on the spectral reflectance of vegetation in semiarid regions. *Remote Sens Environ* 57:88–96
- Karnieli A, Kidron GJ, Glaesser C, Ben-Dor E (1999) Spectral characteristics of cyanobacteria soil crust in semiarid environments. *Remote Sens Environ* 69:67–75
- Karnieli A, Gabai A, Ichoku C, Zaady E, Shachak M (2002) Temporal dynamics of soil and vegetation spectral responses in a semi-arid environment. *Int J Remote Sens* 23:4073–4087
- Karnieli A, Kokaly RF, West NE, Clark RN (2003) Remote sensing of biological soil crusts. In: Belnap J, Lange O (eds) *Biological soil crusts: structure, function, and management*. Springer, Berlin, pp 431–455
- Maestre FT, Quero JL, Gotelli NJ, Escudero A, Ochoa V, Delgado-Baquerizo M et al (2012) Plant species richness and ecosystem multifunctionality in global drylands. *Science* 335:214–218
- Masek J, Vermote E, Saleous N, Wolfe R, Hall F, Huemmrich K, Gao F, Kutler J, Lim TK (2006) A Landsat surface reflectance dataset for North America, 1990–2000. *IEEE Geosci Remote Sens Lett* 3:68–72
- O'Neill AL (1994) Reflectance spectra of microphytic soil crusts in semiarid Australia. *Int J Remote Sens* 15:675–681
- Otterman J (1996) Desert shrub as the cause of reduced reflectance in protected versus impacted sandy arid areas. *Int J Remote Sens* 17:615–619
- Otterman J, Ohring G, Ginzburg A (1974) Results of the Israeli multidisciplinary data analysis of ERTS-1 imagery. *Remote Sens Environ* 3:133–148
- Perold SM (1999) Hepatophyta, part 1: Marchantiopsida, fascicle 1: Marchantiidae. In: Leistner OA (ed) *Flora of Southern Africa*. National Botanical Institute, Pretoria, pp 111–240
- Pinet PC, Kaufmann H, Hill J (2006) Imaging spectroscopy of changing Earth's surface: a major step towards the quantitative monitoring of land degradation and desertification. *Compt Rendus Geosci* 338(14–15):1042–1048
- Pinker RT, Karnieli A (1995) Characteristic spectral reflectance of a semiarid environment. *Int J Remote Sens* 16:1341–1363
- Price JC (1993) Estimating leaf area index from satellite data. *IEEE Trans Geosci Remote Sens* 31(3):727–734
- Raggio J, Pintado A, Vivas M, Sancho LG, Büdel B, Colesie C, Weber B, Schroeter B, Lázaro R, Green TGA (2014) Continuous chlorophyll fluorescence, gas exchange and microclimate monitoring in a natural soil crust habitat in Tabernas badlands, Almeria, Spain: progressing towards a model to understand productivity. *Biodivers Conserv* 23:1809–1826
- Richter R, Schläpfer D (2002) Geo-atmospheric processing of airborne imaging spectrometry data. Part 2: Atmospheric/topographic correction. *Int J Remote Sens* 23:2631–2649
- Rodríguez-Caballero E, Escribano P, Canton Y (2014) Advanced image processing methods as a tool to map and quantify different types of biological soil crust. *ISPRS J Photogramm Remote Sens* 90:59–67
- Rodríguez-Caballero E, Knerr T, Weber B (2015) Importance of biocrusts in dryland monitoring using spectral indices. *Remote Sens Environ* 170:32–39
- Rogge DM, Rivard B, Zhang J, Feng J (2006) Iterative spectral unmixing for optimizing per-pixel endmember sets. *IEEE Trans Geosci Remote Sens* 44:3725–3736
- Rozenstein O, Karnieli A (2014) Identification and characterization of Biological Soil Crusts in a sand dune desert environment across Israel–Egypt border using LWIR emittance spectroscopy. *J Arid Environ* 112:75–86
- Schowengerdt RA (1997) *Remote sensing. Models and methods for image processing*, 3rd edn. Academic, Burlington
- Smith MO, Ustin SL, Adams JB, Gillespie AR (1990) Vegetation in deserts: I. A regional measure of abundance from multispectral images. *Remote Sens Environ* 31:1–26

- Tsoar H, Karnieli A (1996) What determines the spectral reflectance of the Negev-Sinai sand dunes. *Int J Remote Sens* 17:513–525
- Ustin SL, Valko PG, Kefauver SC, Santos MJ, Zimpfer JF, Smith SD (2009) Remote sensing of biological soil crust under simulated climate change manipulations in the Mojave Desert. *Remote Sens Environ* 113:317–328
- Vicente-Serrano SM, Pérez-Cabello F, Lasanta T (2008) Assessment of radiometric correction techniques in analyzing vegetation variability and change using time series of Landsat images. *Remote Sens Environ* 112(10):3916–3934
- Weber B, Olehowski C, Knerr T, Hill J, Deutschewitz K, Wessels DCJ, Eitel B, Büdel B (2008) A new approach for mapping of Biological Soil Crusts in semidesert areas with hyperspectral imagery. *Remote Sens Environ* 112:2187–2201
- Yamano H, Chen J, Zhang Y, Tamura M (2006) Relating photosynthesis of biological soil crusts with reflectance: preliminary assessment based on a hydration experiment. *Int J Remote Sens* 27:5393–5399
- Zaady E, Karnieli A, Shachak M (2007) Applying a field spectroscopy technique for assessing successional trends of biological soil crusts in a semi-arid environment. *J Arid Environ* 70: 463–477